New Journal of Physics
The open-access journal for physics

Exploiting the Poincaré–Bloch symmetry to design high-fidelity broadband composite linear retarders

Arzhang Ardavan
Clarendon Laboratory, Department of Physics, Oxford University, Oxford OX1 3PU, UK
E-mail: arzhang.ardavan@physics.ox.ac.uk

New Journal of Physics **9** (2007) 24
Received 11 September 2006
Published 8 February 2007
Online at http://www.njp.org/
doi:10.1088/1367-2630/9/2/024

Abstract. States can be mapped between the Poincaré space (representing photon polarizations) and the Bloch space (representing states of a quantum spin-$\frac{1}{2}$ particle). Using this mapping and analogous mappings for unitary operators, techniques and formalisms developed in one space can be applied in the other. As an example, error-correction strategies originally developed in the context of pulsed nuclear magnetic resonance experiments are applied to linear optics to propose the design of a new class of composite high-fidelity broadband linear retarder.

The Poincaré sphere provides a convenient representation of the polarization state of a photon or a light ray [1]. Adopting a basis set $|R\rangle$ and $|L\rangle$, representing right- and left-circular polarized photons respectively, a photon of any polarization can be represented (within an overall phase) by the superposition

$$|P\rangle = \cos(\theta/2)\,|R\rangle + \exp(\mathrm{i}\phi)\sin(\theta/2)\,|L\rangle\,. \tag{1}$$

The angles θ and ϕ then define the point on the surface of the unit sphere whose North and South poles represent the states $|R\rangle$ and $|L\rangle$ respectively (see figure 1(a)). Points in the northern (southern) hemisphere represent general right- (left-) elliptical polarizations and the points on

PII: S1367-2630(07)32464-6

the equator represent all possible linear polarizations. The orthogonal horizontal and vertical linear polarizations

$$|H\rangle = \frac{1}{\sqrt{2}}(|R\rangle - |L\rangle) \qquad \text{and} \qquad |V\rangle = \frac{1}{\sqrt{2}}(|R\rangle + |L\rangle), \tag{2}$$

appear at diametric points on the equator, as do the diagonal polarizations

$$|D_+\rangle = \frac{1}{\sqrt{2}}(|R\rangle + \mathrm{i}\,|L\rangle) \qquad \text{and} \qquad |D_-\rangle = \frac{1}{\sqrt{2}}(|R\rangle - \mathrm{i}\,|L\rangle). \tag{3}$$

In general, any two diametric points on the sphere represent a new orthogonal polarization basis, and the arbitrary state in equation (1) can be expressed in this new basis.[1]

When we consider the action of retarders, the power of the Poincaré sphere construction becomes clear. For example, a quarter-wave circular retarder introduces an additional phase of $\pi/2$ to the $|L\rangle$ component over the $|R\rangle$ component, so the retarder converts the state in equation (1) to

$$\mathcal{C}_{\lambda/4}\,|P\rangle = \cos(\theta/2)\,|R\rangle + \exp\,[\mathrm{i}(\phi + \pi/2)]\sin(\theta/2)\,|L\rangle, \tag{4}$$

where $\mathcal{C}_{\lambda/4}$ is an operator representing the action of the plate. In fact, $\mathcal{C}_{\lambda/4}$ is simply a rotation of $\pi/2$ about the axis connecting $|L\rangle$ and $|R\rangle$ in figure 1(a); thus it leaves purely circularly polarized states unchanged, converts vertically or horizontally polarized states to diagonally polarized ones, and so on. Similarly, a linear quarter-wave retarder with its optic axis aligned vertically introduces a phase of $\pi/2$ to the $|V\rangle$ component over the $|H\rangle$ component. The corresponding operator is a rotation of $\pi/2$ about the axis connecting $|H\rangle$ and $|V\rangle$; it rotates linear polarizations onto circular polarizations and vice versa.

In this paper, the following notation will be adopted: $\mathcal{L}_\alpha^\phi$ describes the action of a linear retarder introducing a phase of α to one linear polarization component, with its optic axis at an angle $\phi/2$ to the vertical. In figure 1(a) this operator corresponds to a rotation of an angle α about a horizontal axis that makes an angle ϕ with the axis connecting $|H\rangle$ and $|V\rangle$[2]. Thus a horizontally aligned half-waveplate would be represented by the operator $\mathcal{L}_\pi^{\pm\pi}$, with the choice of sign reflecting the choice of horizontal orientation. In fact, commercial wave plates are typically 'multiple order', meaning that they should actually be represented by $\mathcal{L}_{(2n\pi+\alpha)}^\phi$ where $\alpha = \pi/2$ for a quarter-wave plate and $\alpha = \pi$ for a half-wave plate. 'Zero-order' wave plates are also available, made from two multiple-order plates, and represented by $\mathcal{L}_{2n\pi}^{-\phi} \cdot \mathcal{L}_{(2n\pi+\alpha)}^\phi = \mathcal{L}_\alpha^\phi$.

Given that the polarization state of a photon resides in a two-dimensional state-space, it is not surprising that the Poincaré sphere shares much in common with the Bloch sphere [3], which

[1] The Stokes parameters, an alternative representation of polarization, are given by the projections $S_0 = 2\langle P|P\rangle$, $S_1 = 2(|\langle H|P\rangle|^2 - \langle P|P\rangle)$, $S_2 = 2(|\langle D_+|P\rangle|^2 - \langle P|P\rangle)$ and $S_3 = 2(|\langle R|P\rangle|^2 - \langle P|P\rangle)$ [2].

[2] Adopting the basis defined by $|R\rangle = (1, 0)^T$ and $|L\rangle = (0, 1)^T$, the operator $\mathcal{L}_\alpha^\phi$ can be expressed explicitly in matrix notation as

$$\mathcal{L}_\alpha^\phi = \begin{pmatrix} \cos\left(\frac{1}{2}\alpha\right) & \mathrm{i}\exp(-\mathrm{i}\phi)\sin\left(\frac{1}{2}\alpha\right) \\ \mathrm{i}\exp(\mathrm{i}\phi)\sin\left(\frac{1}{2}\alpha\right) & \cos\left(\frac{1}{2}\alpha\right) \end{pmatrix}. \tag{5}$$

This is the Jones matrix [2] represented in the $|R\rangle$, $|L\rangle$ basis.

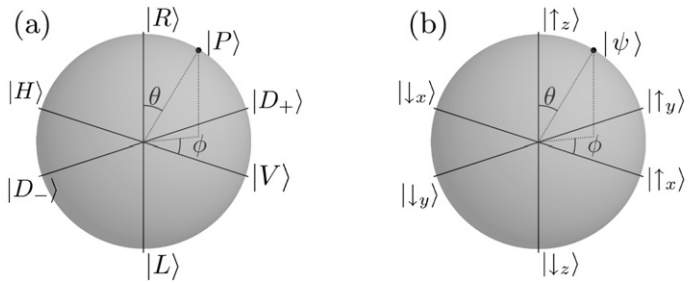

Figure 1. (a) The Poincaré sphere representing all possible polarizations of a photon or light ray. (Polarizations shown: $|R\rangle$, $|L\rangle$, right and left circular; $|H\rangle$, $|V\rangle$, horizontal and vertical; $|D_\pm\rangle$, diagonal.) (b) The Bloch sphere representing all possible quantum states of a two-level system. (Notation: $|\uparrow_i\rangle$ represents a spin-up state along the i-axis.)

is usually invoked to describe the state of a spin-$\frac{1}{2}$ particle but is, in fact, generally applicable to two-level quantum systems. By analogy with equation (1), the general spin-half state,

$$|\psi\rangle = \cos\,(\theta/2)\,|\uparrow_z\rangle + \exp\,(\mathrm{i}\phi)\,\sin\,(\theta/2)\,|\downarrow_z\rangle\,, \tag{6}$$

can be represented as a point on the Bloch sphere; figure 1(b) shows how the polarization states on the Poincaré sphere map onto the spin states on the Bloch sphere. (Of course, other valid mappings exist, but the mapping in figure 1 will be particularly convenient for the following discussion.)

Just as the utility of the Poincaré sphere becomes clear in considering the action of retarders on photons or rays, the Bloch sphere provides a powerful framework in which to visualize the effect of a magnetic field on the spin state of a spin-$\frac{1}{2}$ particle. Applying a magnetic field B along the z-axis generates a Zeeman splitting, $\hbar\omega = \gamma\mu\mathrm{B}$, between the energies of states $|\uparrow_z\rangle$ and $|\downarrow_z\rangle$, where γ is the gyromagnetic ratio and μ is the magnetic moment of the particle. With time, the $|\downarrow_z\rangle$ part of the superposition accumulates a phase with respect to the $|\uparrow_z\rangle$ part at a rate ω; the spin thus 'precesses' about the z-axis [3, 4]. The unitary transformation generated by a z-axis magnetic field applied for a limited duration to a spin-$\frac{1}{2}$ particle is analogous to the action of a circular retarder on a photon. Similarly, a magnetic field applied for a duration $\alpha\hbar/(\gamma\mu\mathrm{B})$ in the $x-y$ plane at an angle ϕ to the x-axis is analogous to the action of a linear retarder represented by the operator $\mathcal{L}_\alpha^\phi$.

In fact, experiments of this kind on spin-$\frac{1}{2}$ systems are more commonly done with a fixed magnetic field applied along the z-axis, such that the moment's state precesses at a rate ω_z. For a transverse field to couple to the moment, it must be circularly polarized at the same frequency, i.e., it must be resonant. This problem is most simply treated by moving into a rotating frame at frequency ω_z [5]. The finite duration transverse magnetic field applied to generate a rotation of the spin's state around a particular transverse axis in the rotating frame corresponds to a pulse of radiation of frequency ω_z in the lab frame: the pulse duration and intensity determine the angle through which the state is rotated; the phase of the pulse determines about which axis in the rotating frame the rotation occurs. Such 'pulsed magnetic resonance' experiments are most commonly performed on large ensembles of nuclear magnetic moments [5] and electron paramagnetic moments [6].

To summarize, each possible polarization state for a photon, represented by a point on the Poincaré sphere, maps on to a state of a spin-$\frac{1}{2}$ particle, represented by a point on the Bloch sphere. The action of a linear retarder on a photon is to rotate the state of polarization about an axis in the horizontal plane of figure 1(a); the equivalent operation on the state of a spin-$\frac{1}{2}$ particle is the application of a radiation pulse of appropriate duration and phase. Given this symmetry between the properties of states and operations defined in the Poincaré and Bloch spaces, we may now consider the possibility of applying the formalisms and techniques developed for one space in the other.

For example, various techniques have been developed by magnetic resonance spectroscopists to address certain kinds of systematic error that arise in pulsed magnetic resonance experiments. One class, rotation angle errors, can arise because the ensemble of spins constituting the sample is distributed over a finite volume. The experiments are typically performed in a resonator to enhance the intensity of the radiation coupling to the spins. Depending on the geometry of the resonator and the size of the sample, the intensity of the radiation can vary significantly over the volume occupied by the sample, and this variation leads to a distribution of rotation angles across the sample. Errors of this kind are systematic in the sense that a particular spin 'overshoots' or 'undershoots' by the same factor each time a radiation pulse is applied, because its position within the resonator does not change. Using the notation described above, a pulse might be applied with the intention of generating the rotation described by $\mathcal{L}_{\alpha}^{\phi_0}$, but the rotation that actually takes place is $\mathcal{L}_{(1+\epsilon)\alpha}^{\phi_0}$. The fact that, for a particular spin, the error ϵ is the same in successive pulses (i.e. the error is systematic) can be exploited to develop methods for correcting it [7].

The strategy (known in the magnetic resonance literature as BB1 [7] or W1 [8]) is to apply a sequence of corrective operators after the initial 'naïve' operator, so the composite sequence becomes

$$\mathcal{L}_{\mathrm{C}}(\alpha, \phi_0, \phi_1, \phi_2, \epsilon) = \mathcal{L}_{(1+\epsilon)\pi}^{\phi_1} \cdot \mathcal{L}_{2(1+\epsilon)\pi}^{\phi_2} \cdot \mathcal{L}_{(1+\epsilon)\pi}^{\phi_1} \cdot \mathcal{L}_{(1+\epsilon)\alpha}^{\phi_0}, \tag{7}$$

where ϕ_1 and ϕ_2 are to be chosen to optimize the performance of the composite sequence. This is facilitated by defining a quantity called the fidelity of two unitary operators A and B,

$$\mathcal{F}(A, B) = \tfrac{1}{2}\mathrm{Tr}(A^{-1} \cdot B). \tag{8}$$

The fidelity has the following properties: if the two operators, A and B, are identical, $\mathcal{F} = 1$; as the rotations that they represent deviate from one another, $\mathcal{F}$ decreases. The fidelity is thus a useful measure of how similar the composite operator $\mathcal{L}_{\mathrm{C}}$ is to the ideal operator $\mathcal{L}_{\alpha}^{\phi_0}$. We proceed by expanding the fidelity of these operators in powers of the rotation angle error, ϵ,

$$\mathcal{F}(\mathcal{L}_{\mathrm{C}}, \mathcal{L}_{\alpha}^{\phi_0}) = 1 - \mathcal{F}_2\epsilon^2 - \mathcal{F}_4\epsilon^4 - \mathcal{F}_6\epsilon^6 - \cdots, \tag{9}$$

where the coefficients $\mathcal{F}_i$ are functions of α, $\phi_1 - \phi_0$ and $\phi_2 - \phi_0$. The coefficients of odd powers of ϵ are zero because the fidelity is an even function of the error; $\mathcal{F}$ can only decrease from 1 as the errors increase. The final step is to choose values of ϕ_1 and ϕ_2 such that the leading terms in the expansion of $\mathcal{F}$ become zero. In practice, this approach is very successful, and it is always possible to suppress the coefficients $\mathcal{F}_2$ and $\mathcal{F}_4$. The fidelity of the composite operator $\mathcal{L}_{\mathrm{C}}$ thus

Table 1. Commonly encountered examples of the operator $\mathcal{L}_{\alpha}^{\phi}$, the corresponding experimental operations in the Poincaré and Bloch spaces, and the values of ϕ_0, ϕ_1 and ϕ_2 for the BB1 composite operator.

Operator	Poincaré operation	Bloch operation	ϕ_0	$\phi_1 - \phi_0$	$\phi_2 - \phi_0$
$\mathcal{L}_{\pi/2}^{0}$	$\frac{1}{4}$-waveplate (optic axis vertical)	$\pi/2$-pulse around x-axis	0	4.587	1.195
$\mathcal{L}_{\pi/2}^{\pi/2}$	$\frac{1}{4}$-waveplate (optic axis diagonal)	$\pi/2$-pulse around y-axis	$\pi/2$	4.587	1.195
$\mathcal{L}_{\pi}^{0}$	$\frac{1}{2}$-waveplate (optic axis vertical)	π-pulse around x-axis	0	4.460	0.8128
$\mathcal{L}_{\pi}^{\pi/2}$	$\frac{1}{2}$-waveplate (optic axis diagonal)	π-pulse around y-axis	$\pi/2$	4.460	0.8128

depends on the fractional error ϵ only to the sixth power. To optimize a rotation of α about an axis defined by ϕ_0, ϕ_1 and ϕ_2 are found to be [8, 9]

$$\phi_1 - \phi_0 = \pm\arccos\left(-\frac{\alpha}{4\pi}\right) \qquad \text{and} \qquad \phi_2 - \phi_0 = 3(\phi_1 - \phi_0). \tag{10}$$

(Recently, Brown *et al* have generalized the BB1 approach to correct errors to *arbitrary* order in ϵ [10]. However, they find that to improve at all on BB1 a very large number of corrective pulses are required; it is not yet clear whether such long corrective sequences will be useful in practice.)

Two points are worth highlighting at this stage. Firstly, this procedure corrects the *operator*, not the state. $\mathcal{L}_{\mathrm{C}}$ thus constitutes a better approximation to the ideal operator *independently of the starting state*. Secondly, although the strategy outlined here was developed in the context of pulsed magnetic resonance, and has been shown to be very effective in both nuclear [7] and electron [11] resonance experiments, the formalism is equally applicable to rotations of the polarization of a photon. The practical device that can implement the operation $\mathcal{L}_{\mathrm{C}}$ in the Poincaré space is a composite stack of four zero-order linear waveplates, whose optic axes have specific relative orientations defined by ϕ_0, ϕ_1 and ϕ_2, replacing the single waveplate. Table 1 lists BB1 solutions for ϕ_1 and ϕ_2 for common rotations, and descriptions of the corresponding waveplates or radiation pulses.

In order to appreciate fully the benefits of the composite retarder, we must consider the source of the rotation angle error, ϵ, that it corrects. A conventional zero-order retarder must be constructed for a specific wavelength, λ_0; the thickness of the waveplate must be such that the relative phase accumulated by the two polarization components is $\pi/2$ (for a quarter-waveplate) or π (for a half-waveplate). If the actual wavelength λ deviates from λ_0, the effective path length through the plate changes, and the relative phase accumulated is wrong by a factor

$$(1 + \epsilon) = \lambda_0/\lambda. \tag{11}$$

Thus the rotation angle error, given by the fractional change in the wavelength, is systematic in the same way as the errors described above for spin-$\frac{1}{2}$ systems. Having shown that the fidelity of the composite operator $\mathcal{L}_{\mathrm{C}}$ is less sensitive to rotation angle errors of this kind than the simple rotation, it is interesting to examine the effect that this has on the practical utility of the composite

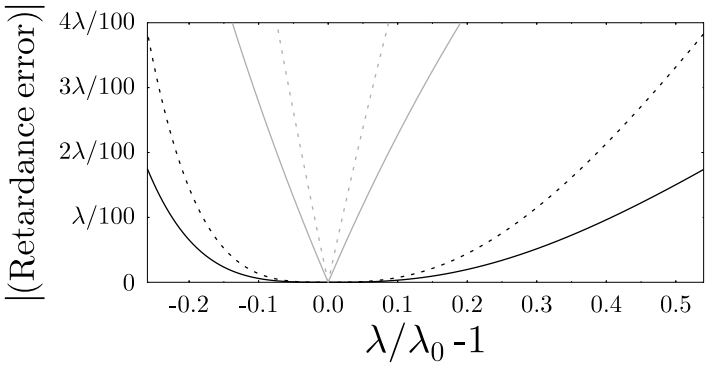

Figure 2. In black, the magnitude of the retardance error for (solid) quarter-wave and (dashed) half-wave BB1 composite retarders as a function of the fractional deviation of the wavelength from the designated wavelength, λ_0. In grey, the same quantities for simple zero-order waveplates.

retarder over a conventional zero-order retarder. The fidelity of the conventional retarder depends on the rotation angle error as ϵ,

$$\mathcal{F}\left(\mathcal{L}^{\phi_0}_{(1+\epsilon)\alpha}\cdot\mathcal{L}^{\phi_0}_{\alpha}\right)=\cos\left(\frac{\alpha\epsilon}{2}\right)\approx 1-\frac{\alpha^2\epsilon^2}{4}, \tag{12}$$

for small values of ϵ. Therefore, if, for a particular application, an effective rotation error of $\epsilon_{\max}$ is tolerable, the maximum actual fractional error that can be sufficiently corrected by the composite retarder, $\epsilon^{\mathrm{C}}_{\max}$, satisfies

$$\mathcal{F}_6\left(\epsilon^{\mathrm{C}}_{\max}\right)^6=\frac{\alpha^2\epsilon^2_{\max}}{4}\qquad\text{or}\qquad\epsilon^{\mathrm{C}}_{\max}=\left(\frac{\alpha^2}{4\mathcal{F}_6}\right)^{1/6}\sqrt[3]{\epsilon_{\max}}, \tag{13}$$

for small values of $\epsilon_{\max}$ and $\epsilon^{\mathrm{C}}_{\max}$. $\mathcal{F}_6$ depends on the target rotation angle α, but in the range $0<\alpha\leqslant\pi$, $|\mathcal{F}_6|<5$. Thus for example, under the circumstances where a conventional quarter-wave retarder (for which $\alpha=\pi/2$ and $\mathcal{F}_6\approx 1$) would function satisfactorily over a range of wavelengths within $\pm 0.1\%$ of its designated wavelength, the composite retarder would work over a range exceeding $\pm 11\%$. For larger tolerable errors, the small-ϵ approximation breaks down. Figure 2 shows the magnitude of the retardance error of quarter- and half-wave BB1 composite retarders as a function of the fractional deviation of the wavelength from the designated value, λ_0. The retardance error remains small over a remarkably large wavelength bandwidth compared to traditional zero-order retarders.

For applications where a very large bandwidth is important but small errors over the whole range can be tolerated, a second, related, class of composite rotation, known as BB2 [7], is more suitable. In the BB2 sequence $\phi_1-\phi_0=\pi/2$ is fixed, and the choice of ϕ_2 depends on the bandwidth required and the error that can be tolerated. Figure 3 shows the magnitude of the retardance error for quarter- and half-wave retarders with ϕ_2 chosen such that the retardance error does not exceed $\lambda/20$. The wavelength range over which the retardation error is below $\lambda/20$ is extremely wide: $0.6\lambda_0<\lambda<3.2\lambda_0$ for the quarter-wave retarder and $0.65\lambda_0<\lambda<2.2\lambda_0$ for the half-wave retarder.

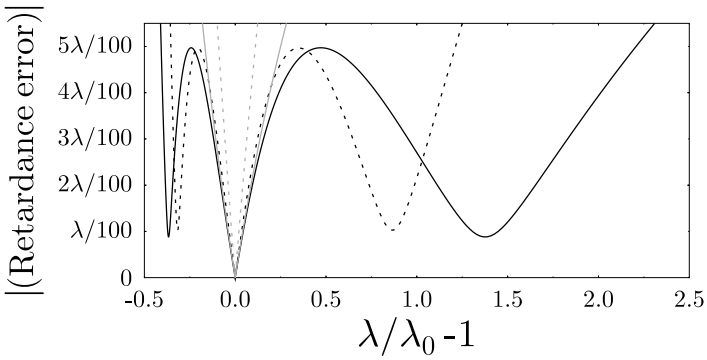

Figure 3. In black, the magnitude of the retardance error for (solid) quarter-wave and (dashed) half-wave BB2 composite retarders as a function of the fractional deviation of the wavelength from the designated wavelength, λ_0. For the quarter-waveplate, $\phi_1 - \phi_0 = \pi/2$, $\phi_2 - \phi_0 = 5.19$; for the half-waveplate, $\phi_1 - \phi_0 = \pi/2$, $\phi_2 - \phi_0 = 5.43$. In grey, the same quantities for simple zero-order waveplates.

Finally, we must consider the practicality of building a composite retarder. The device comprises a sequence of conventional retarders with relative alignments determined by the intended action of the composite retarder. Given that it is impossible to build the composite with ideal components and perfect alignments, the operator for a practical retarder is (cf the operator representing the ideal device, see equation (6)).

$$\mathcal{L}_{C,\mathrm{imp}} = \mathcal{L}^{\phi_1+\delta\phi_1}_{(1+\epsilon+\delta_1)\pi} \cdot \mathcal{L}^{\phi_2+\delta\phi_2}_{2(1+\epsilon+\delta_2)\pi} \cdot \mathcal{L}^{\phi_1+\delta\phi_3}_{(1+\epsilon+\delta_3)\pi} \cdot \mathcal{L}^{\phi_0+\delta\phi_4}_{(1+\epsilon+\delta_4)\alpha} \tag{14}$$

where the δ_i are caused by errors in the waveplate thicknesses and the $\delta\phi_i$ represent errors in relative alignments. The fidelity $\mathcal{F}(\mathcal{L}_C, \mathcal{L}^{\phi_0}_{\alpha})$ depends on δ_i to second order, and to $\delta\phi_i$ to first order with coefficients smaller than 10^{-3}. The fabrication of the composite retarder is therefore entirely feasible; manufacturing errors would have to be substantial to affect its performance significantly.

Another approach to making waveplates that are less sensitive to wavelength is to combine two waveplates made of materials with different birefringences [12]. The BB1 and BB2 composite retarders described here almost always outperform commercial 'achromatic waveplates' of this kind[3]. By incorporating a larger number of birefringent materials, it is, in principle, possible to improve the performance of multi-material achromatic waveplates [13, 14], but they must be designed individually for particular wavelength ranges, become very sensitive to the precision of construction, and are limited in damage threshold by the weakest constituent material.

A generic problem with compound waveplates is the possibility of interference fringes arising from reflections at interfaces within the stack. This issue is expected to be less severe for constructions of multiple plates of the same material with their optic axes rotated with respect to one another (as described here and elsewhere [15, 16]) than for waveplates constructed from multiple materials of different birefringences. Interference effects in both classes of waveplates have been studied in detail elsewhere [17]–[19].

[3] For example, Tower Optical Corp., 3600 South Congress Ave., Unit J, Boynton Beach, FL 33426, USA, product numbers AO12A-1/4-X (quarter-wave) and AO12A-1/2-X (half-wave).

In summary, states and operators map between the Poincaré and Bloch spaces representing photon polarizations and spin-$\frac{1}{2}$ states respectively. This mapping allows us to translate strategies for control and manipulation of systems that reside in one space into systems residing in the other. In this paper, this is demonstrated by considering the linear-optics analogue of certain classes of pulse sequence developed for nuclear magnetic resonance experiments, and using it to propose the design of a new class of broadband linear retarders with very favourable characteristics.

Acknowledgments

I thank Professor John Rarity for asking an interesting question and Professor S J Blundell for comments on the manuscript. I thank the Royal Society and the EPSRC Quantum Information Processing IRC (GR/S15808/01) for support.

References

[1] Poincaré J H 1889 *Théorie Mathématique de la Lumière* (Paris: Saint-Andre-des-Arts)
[2] Hecht E 2002 *Optics* 4th edn (London: Addison Wesley)
[3] Neilsen M A and Chuang I L 2000 *Quantum Computation and Quantum Information* (Cambridge: Cambridge University Press)
[4] Sakurai J J 1985 *Modern Quantum Mechanics* (Redwood City: Addison Wesley)
[5] Abragam A 1961 *The Principles of Nuclear Magnetism* (Oxford: Oxford University Press)
[6] Schweiger A and Jeschke G 2001 *Principles of Pulse Electron Spin Resonance* (Oxford: Oxford University Press)
[7] Wimperis S 1994 *J. Magn. Reson.* A **109** 221
[8] Cummins H K, Llewellyn G and Jones J A 2003 *Phys. Rev.* A **67** 042308
[9] Hugh D M and Twamley J 2005 *Phys. Rev.* A **71** 012327
[10] Brown K R, Harrow A W and Chuang I L 2004 *Phys. Rev.* A **70** 052318
[11] Morton J J L, Tyryshkin A M, Ardavan A, Porfyrakis K, Lyon S A and Briggs G A D 2005 *Phys. Rev. Lett.* **95** 200501
[12] Clarke D 1967 *Opt. Acta* **14** 343
[13] Hariharan P 1998 *Meas. Sci. Technol.* **9**
[14] Hariharan P 2002 *Opt. Laser Technol.* **34**
[15] Pancharatnam S 1955 *Proc. Indian Acad. Sci.* A **41**
[16] Serkowski K 1976 *Methods of Experimental Physics (Astrophysics: Part A – Optical and Infrared)* vol 12 ed M Meeks and N Carleton (New York: Academic)
[17] Clarke D 2004 *J. Opt. A: Pure Appl. Opt.* **6** 1036
[18] Clarke D 2004 *J. Opt. A: Pure Appl. Opt.* **6** 1041
[19] Clarke D 2004 *J. Opt. A: Pure Appl. Opt.* **6** 1047